Title
Variable-temperature, variable-field magnetic circular dichroism spectroscopic study of NifEN-bound precursor and “FeMoco”

Journal
JBIC Journal of Biological Inorganic Chemistry, 16(2)

ISSN
1432-1327

Authors
Rupnik, Kresimir
Hu, Yilin
Fay, Aaron W.
et al.

Publication Date
2011-02-01

DOI
10.1007/s00775-010-0728-9

Peer reviewed

J Biol Inorg Chem (2011) 16:325–332
DOI 10.1007/s00775-010-0728-9

ORIGINAL PAPER

Variable-temperature, variable-field magnetic circular dichroism spectroscopic study of NifEN-bound precursor and "FeMoco"

Kresimir Rupnik · Yilin Hu · Aaron W. Fay · Markus W. Ribbe · Brian J. Hales

Received: 8 September 2010 / Accepted: 20 October 2010 / Published online: 1 November 2010

Abstract NifEN plays a key role in the biosynthesis of the iron–molybdenum cofactor (FeMoco) of nitrogenase. A scaffold protein that hosts the conversion of a FeMoco precursor to a mature cofactor, NifEN can assume three conformations during the process of FeMoco maturation. One, designated Δ*nifB* NifEN, contains only two permanent $[Fe_4S_4]$-like clusters. The second, designated $NifEN^{Precursor}$, contains the permanent clusters and a precursor form of FeMoco. The third, designated $NifEN^{"FeMoco"}$, contains the permanent $[Fe_4S_4]$-like clusters and a fully complemented, "FeMoco"-like structure. Here, we report a variable-temperature, variable-field magnetic circular dichroism spectroscopic investigation of the electronic structure of the metal clusters in the three forms of dithionite-reduced NifEN. Our data indicate that the permanent $[Fe_4S_4]$-like clusters are structurally and electronically conserved in all three NifEN species and exhibit spectral features of classic $[Fe_4S_4]^{+}$ clusters; however, they are present in a mixed spin state with a small contribution from the $S > ½$ spin state. Our results also suggest that both the precursor and "FeMoco" have a conserved Fe/S electronic structure that is similar to the electronic structure of FeMoco in the MoFe protein, and that the "FeMoco" in $NifEN^{"FeMoco"}$ exists, predominantly, in an $S = 3/2$ spin state with spectral parameters identical to those of FeMoco in the MoFe protein. These observations provide strong support to the outcome of our previous EPR and X-ray absorption spectroscopy/extended X-ray absorption fine structure analysis of the three NifEN species while providing significant new insights into the unique electronic properties of the precursor and "FeMoco" in NifEN.

Keywords Cofactor · Iron–sulfur cluster · Magnetic circular dichroism · Metallocenter assembly

Abbreviations

CD	Circular dichroism
EXAFS	Extended X-ray absorption fine structure
FeMoco	Fe–Mo cofactor
MCD	Magnetic circular dichroism
MoFe	Mo–Fe
Tris	Tris(hydroxymethyl)aminomethane
XAS	X-ray absorption spectroscopy

Introduction

Nitrogenase is a complex metalloenzyme that catalyzes the nucleotide-dependent reduction of atmospheric N_2 to bioavailable NH_3. The best-studied Mo-dependent nitrogenase is a binary system consisting of the Fe protein and the Fe–Mo (MoFe) protein [1]. The Fe protein is an α_2 homodimer containing one $[Fe_4S_4]$ cluster at the subunit interface and one MgATP binding site within each subunit [2], whereas the MoFe protein is an $\alpha_2\beta_2$ heterotetramer containing one P-cluster ($[Fe_8S_7]$) at each α/β-subunit

K. Rupnik · B. J. Hales (✉)
Department of Chemistry,
Louisiana State University,
Baton Rouge, LA 70803, USA
e-mail: bhales@lsu.edu

Y. Hu · A. W. Fay · M. W. Ribbe (✉)
Department of Molecular Biology and Biochemistry,
University of California,
Irvine, CA 92697, USA
e-mail: mribbe@uci.edu

interface and one Fe–Mo cofactor (FeMoco) ([$MoFe_7S_9X$-homocitrate], where X is C, N, or O) within each α subunit [3]. During catalysis, the Fe protein serves as an obligate electron donor for the MoFe protein and, in an ATP-dependent process, mediates the transfer of electrons from its [Fe_4S_4] cluster, through the P-cluster, to the FeMoco of the MoFe protein, where substrate reduction eventually occurs [1, 4].

Biosynthesis of FeMoco has remained a central topic in the field of bioinorganic chemistry because of its complexity and intricacy [5]. This process is presumably initiated by the mobilization of Fe and S by NifU (encoded by *nifU*) and NifS (encoded by *nifS*) for the assembly of small Fe/S fragments, which are subsequently used for the generation of an Fe/S core on NifB (encoded by *nifB*). Such an Fe/S core, which likely contains all Fe and S required for the formation of the mature cofactor, is then transferred to NifEN (encoded by *nifE* and *nifN*), where it is further matured before being delivered to its binding site in the MoFe protein [6]. The hypothesis that NifEN is a scaffold protein for FeMoco assembly is largely based on the significant sequence homology between NifEN and MoFe protein. Comparison between the primary sequences of these two proteins has led to the proposal that NifEN contains a "P-cluster site" that houses a P-cluster homolog and a "FeMoco site" that hosts the conversion of FeMoco precursor to a mature cofactor [6]. Although the P-cluster homolog was identified as an [Fe_4S_4]-type cluster earlier [7], the FeMoco precursor was identified only recently [8, 9] following the biochemical/spectroscopic characterization of two forms of NifEN from *Azotobacter vinelandii*: one, designated Δ*nifB* NifEN, contains an [Fe_4S_4] cluster at the "P-cluster site" but no FeMoco species at the "FeMoco site"; the other, designated $NifEN^{Precursor}$, contains an [Fe_4S_4] cluster at the "P-cluster site" and a precursor form of FeMoco at the "FeMoco site" (Fig. 1). Subtractive X-ray absorption spectroscopy (XAS)/extended X-ray absorption fine structure (EXAFS) analysis revealed that the precursor on $NifEN^{Precursor}$ is a Mo/homocitrate-free cluster that closely resembles the Fe/S core of FeMoco [9]. Furthermore, combined biochemical and XAS/EXAFS investigations showed that, in an ATP- and reductant-dependent process, Fe protein can insert Mo and homocitrate into the NifEN-bound precursor, leading to the formation of a third form of NifEN (designated $NifEN^{"FeMoco"}$), which contains a fully complemented "FeMoco" that can directly activate the FeMoco-deficient Δ*nifB* MoFe protein [10–12].

EPR spectroscopy has yielded information regarding the spin states of the different clusters of the three NifEN species, which complements the structural information generated by XAS/EXAFS analysis. However, neither technique has revealed information necessary for the complete characterization of the electronic structures of the clusters. To elucidate the electronic structures of the NifEN-associated clusters, we performed a variable-temperature, variable-field magnetic circular dichroism (MCD) investigation of the three forms of NifEN in the dithionite-reduced state. The results reported herein provide the electronic information of the NifEN-associated clusters that is necessary for a better understanding of the maturation process of FeMoco.

Materials and methods

Unless noted otherwise, all chemicals and reagents were obtained from Fisher Scientific or Sigma–Aldrich.

Cell growth and protein purification

Wild-type (AvOP) and variant (DJ1041 and YM9A) strains of *A. vinelandii* were used in this study. DJ1041 expresses a His-tagged NifEN (designated $NifEN^{Precursor}$) in the *nifHDKTY*-deletion background, and YM9A expresses a His-tagged NifEN (designated Δ*nifB* NifEN) in the *nifHDKTY/nifB*-deletion background [7, 8]. All *A. vinelandii* strains were grown in 180-L batches in a 200-L New Brunswick fermentor (New Brunswick Scientific, Edison, NJ, USA) in Burke's minimal medium supplemented with

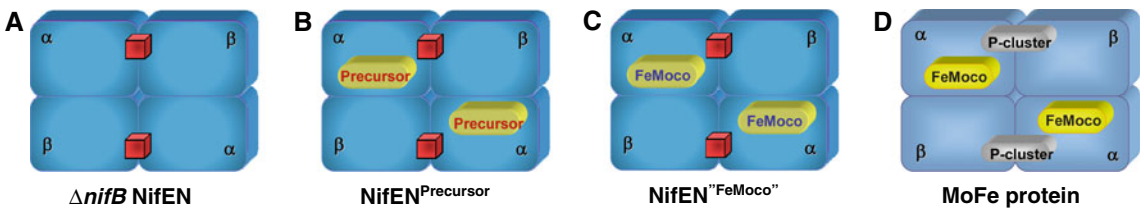

Fig. 1 The $\alpha_2\beta_2$-heterotetrameric Δ*nifB* NifEN (**a**), $NifEN^{Precursor}$ (**b**), $NifEN^{"FeMoco"}$ (**c**), and MoFe protein (**d**). The permanent [Fe_4S_4] clusters of NifEN at the αβ-subunit interfaces are indicated by *red cubes*. Compared with Δ*nifB* NifEN, $NifEN^{Precursor}$, and $NifEN^{"FeMoco"}$ contain additional clusters within the αβ subunits (i.e., precursor and "FeMoco", respectively), which are indicated by *yellow ovals*. The MoFe protein contains one [Fe_8S_7] P-cluster at each αβ-subunit interface (*gray ovals*) and one FeMoco within each α subunit (*yellow oval*)

2 mM ammonium acetate. The growth rate was measured by cell density at 436 nm using a Spectronic 20 Genesys (Spectronic Instruments, Westbury, NY, USA). After the consumption of ammonia, the cells were derepressed for 3 h, followed by harvesting using a flow-through centrifugal harvester (Cepa, Lahr, Germany). The cell paste was washed with 50 mM tris(hydroxymethyl)aminomethane (Tris)–HCl (pH 8.0). Published methods were used for the purification of wild-type *A. vinelandii* Fe protein [13] and His-tagged NifEN [8].

Protein sample preparation

Three forms of NifEN were used in the comparative MCD studies: (1) Δ*nifB* NifEN, which contains one [Fe_4S_4] cluster at each "P-cluster site" of NifEN; (2) $NifEN^{Precursor}$, which contains, in addition to the [Fe_4S_4] clusters at the "P-cluster sites", a FeMoco precursor at the "FeMoco site" of NifEN; and (3) $NifEN^{"FeMoco"}$, which contains the [Fe_4S_4] clusters at the "P-cluster sites" and a fully complemented "FeMoco" at the "FeMoco site" of NifEN. $NifEN^{"FeMoco"}$ was obtained by incubating $NifEN^{Precursor}$ with Fe protein, MgATP, dithionite, sodium molybdate (Na_2MoO_4), and homocitrate, and reisolating NifEN following such treatment [10, 11]. All MCD samples were prepared in an Ar-filled drybox (Vacuum Atmospheres, Hawthorne, CA, USA) at an oxygen level of less than 4 ppm [14]. Dithionite-reduced protein samples were in 25 mM Tris–HCl (pH 8.0), 10% glycerol, and 2 mM dithionite ($Na_2S_2O_4$). Samples were subsequently concentrated in a Centricon-50 concentrator (Amicon) in anaerobic centrifuge tubes outside the drybox as described earlier [15]. After concentration, these protein samples [50–100 mg mL^{-1} in 25 mM Tris–HCl (pH 8.0) and 50% glycerol] were transferred to MCD sample cuvettes under anaerobic conditions and frozen in liquid N_2. MCD sample cells were constructed from optical-quality Spectrosil® quartz (170–2,200 nm, 1-mm path length, model BS-1-Q-1, Starna®, model SUV R-1001 or FUV; Spectrocell, Oreland, PA, USA). Each cuvette was cut into the appropriate dimensions to fit the sample holder (2.0 cm × 12.5 mm), resulting in a sample volume of approximately 160 μL. All samples contained 50% glycerol to ensure the formation of an optical glass upon freezing and were kept on dry ice in transit.

Spectroscopic characterization

MCD spectra were recorded with a circular dichroism (CD) spectropolarimeter (model J-710; JASCO, Easton, MD, USA) interfaced with a superconducting magnet (model Spectromag 400-7T; Oxford Instruments, Oxford, UK) as previously described [14]. Sample temperatures were monitored with a thin film resistance temperature sensor (model CX1050-Cu-1-4L; Lakeshore, Westerville, OH, USA) positioned directly (1 mm) above the sample cuvette. The linearity of the magnetic field was monitored with a calibrated Hall generator (model HGCA-3020; Lakeshore, Westerville, OH, USA) placed directly outside the superconducting magnet.

MCD spectra were recorded at a rate of 50 nm min^{-1} from 800 to 350 nm at a resolution of 2–10 nm. Since optical glasses formed at low temperature often generate a strain-induced background CD spectrum, the CD spectrum was recorded in a zero magnetic field to determine whether the background signal was excessive (if it was excessive, the sample was replaced with a new sample). To further eliminate interference by this signal, the corrected MCD spectrum was obtained for each sample by first recording the spectrum with the magnetic field in the normal direction and subtracting from it the spectrum with the field in the reversed direction. All spectral intensities were quantified per $\alpha\beta$ heterodimer and corrected for path length, sample concentration, and depolarization effects. The extent of depolarization was determined by placing a standard sample of nickel tartarate between the magnet cryostat and the detector. The CD spectrum was then recorded before and after light had passed through the frozen protein sample in the magnet.

EPR spectra and metal determinations of the different samples were conducted as previously described [12]. The quantitative results of these analyses are specified in the text for each protein studied.

Analysis of magnetization data

Magnetization curves were recorded at a set wavelength and temperature while the magnetic field was linearly varied from 0 to 6 T at a rate of 0.45 T min^{-1} with a resolution of 2 s. MCD data were analyzed using a fit/simulation program created by Neese and Solomon [16]. The program allows the calculation of best-fit saturation magnetization curves using experimental data as a basis set and is valid for any spin state, half-integer or integer, at any specified temperature.

Experimental data were analyzed by fitting the spin Hamiltonian parameters and the effective transition moment products. The effective transition moment products represent the planes of polarization that reflect the anisotropy of the g factors. Since the initial slope of the magnetization curve is dependent on the g factors, the transition polarizations relate the transition dipole to the g-factor axes of a powder or randomly oriented sample. For $S > ½$ spin systems, the spin parameters, including the g factor (g), the axial zero-field splitting (D) and the rhombic distortion of the electronic environment (E/D), are determined on the basis of the Hamiltonian

$$\hat{H} = \beta B g \hat{S} + D\left[\hat{S}_z^2 - (1/3)\hat{S}(\hat{S}+1) + (E/D)\left(\hat{S}_x^2 - \hat{S}_y^2\right)\right] \quad (1)$$

which is the expression for the energy of the Zeeman interaction and the correction to the energy of the individual spin states arising from spin–orbit coupling. At low temperatures (approximately 1.6 K), the lowest energy level is predominantly populated and dictates the behavior of the magnetization curve. As the temperature is raised, the spectral parameters of excited states become increasingly important in the profile of the magnetization curve. Best-fit simulations of the experimental data were initially performed at the lowest temperature to enable the determination of the spectral parameters. Subsequent simulations of high-temperature data facilitated the determination of the axial zero-field splitting, D.

Results and discussion

The precursor-free Δ*nifB* NifEN has a metal content of eight Fe per $\alpha_2\beta_2$ tetramer. As shown in the past [12], the EPR spectrum of this protein shows a single g 2 signal of an $S = ½$ spin system at a concentration of approximately two spins per tetramer. High-resolution MCD spectra of the Δ*nifB* NifEN at high field (6 T) and various temperatures (1.57, 4.20, and 10.5 K) are shown in Fig. 2. These spectra exhibit two broad positive inflections at 520 and 764 nm, respectively, and a broad negative inflection at 660 nm with a shoulder at 610 nm. This pattern of inflections is characteristic of $[Fe_4S_4]^+$ clusters [17], which exhibit broad positive inflections in the 520–530- and 740–780-nm regions and broad negative inflections in the 620- and 660-nm regions. The 520–530-nm region is associated with the S → Fe^{3+} charge-transfer region [18, 19], whereas the 740–780-nm region has been attributed to a valence-delocalized intervalence band [20]. The intensity at 520 nm (75 $\Delta\varepsilon$ M^{-1} cm^{-1} per $\alpha\beta$ dimer) is well within the average range of intensity (60–90 $\Delta\varepsilon$ M^{-1} cm^{-1}) for a single $[Fe_4S_4]^+$ cluster [21, 22]. All of the analyses are consistent with reduced Δ*nifB* NifEN containing two permanent $[Fe_4S_4]^+$-like clusters (one cluster per $\alpha\beta$ dimer) [7, 8].

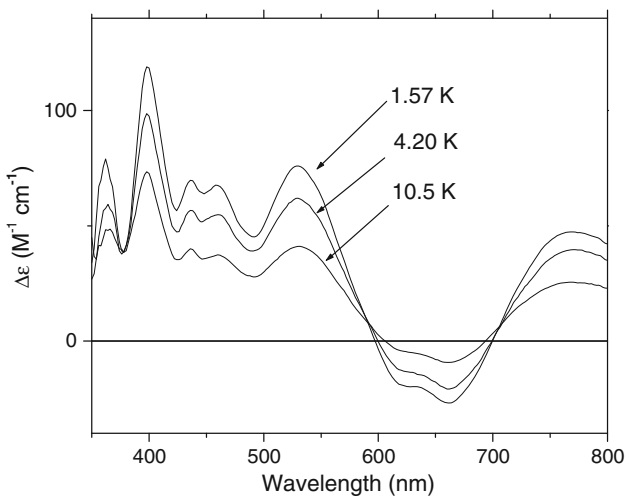

Fig. 2 Magnetic circular dichroism (MCD) spectra of Δ*nifB* NifEN at 6 T and 1.57, 4.20, and 10.5 K

In addition to the "classic" broad MCD inflections of the $[Fe_4S_4]^+$ clusters, four sharp positive inflections at 360, 396, 430, and 458 nm can also be observed in the spectra of Δ*nifB* NifEN. The temperature dependency of these sharp inflections (Fig. 2) parallels that of the broad inflections, implying that all of them arise from the same cluster in the protein. Unlike the broad long-wavelength features, the sharp short-wavelength inflections are not characteristic of all $[Fe_4S_4]^+$ clusters and, therefore, represent an identifying fingerprint of the specific permanent $[Fe_4S_4]^+$-like clusters in Δ*nifB* NifEN.

The $[Fe_4S_4]^+$-like clusters in Δ*nifB* NifEN were further characterized by examining the magnetization of this protein at various temperatures (1.57, 4.20, and 10.5 K) (Fig. 3). The EPR spectrum of Δ*nifB* NifEN exhibits a dominant $S = ½$ signal in the g 2 region [8]. It is obvious that the experimental magnetization curves do not mimic the simulated curve for the pure $S = ½$ system. First, the 1.57 K magnetization curve does not approach a horizontal (i.e., saturation) limit at high magnetic field. This observation suggests the presence of a small B term (i.e., diamagnetic) and/or high-spin contribution to the spectral

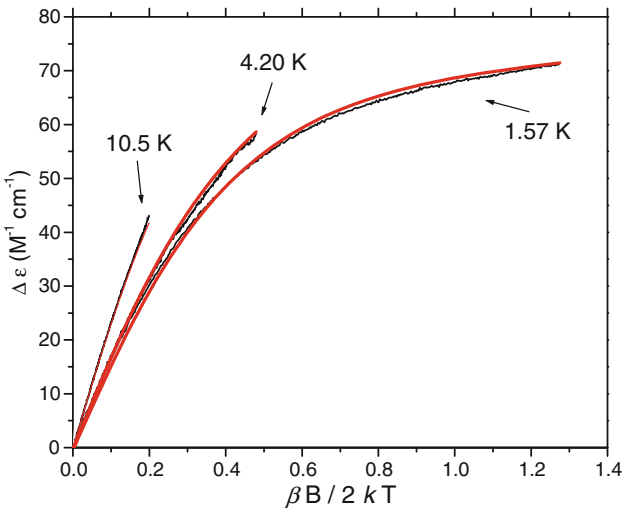

Fig. 3 Magnetization curves of Δ*nifB* NifEN at 1.57, 4.20, and 10.5 K (*black*) recorded at 520 nm and an example of a possible simulation (*red*) of the magnetization curves assuming a mixture of an $S = ½$ spin system (65%) with g [2.07, 1.91, 1.84] and an $S = 3/2$ spin system (30%) with $E/D = 0.052$ and $D = 5.0$ cm^{-1} (polarizations used in simulations $M_{xy} = 1.0$, $M_{xz} = 1.0$, $M_{yz} = 1.0$) and a 5% linear B term

intensity. A *B*-term contribution is typically temperature-independent with a near-linear increase in intensity upon an increase in field. Second, there is a nesting of the magnetization data at high temperatures. Nesting is the flaring of the magnetization curves as the temperature increases and often occurs in higher-spin states (i.e., $S > ½$), where low-lying, excited-levels (with different magnetization parameters) become populated as the temperature increases (Eq. 1). Nesting is not observed in the case of a pure $S = ½$ system, where there are no low-lying excited states. Both the MCD spectral pattern and the magnetization data are similar to those observed in another NifEN species that is practically free of precursor [7].

The magnetization data of Δ*nifB* NifEN, therefore, suggest the presence of an additional high-spin state in this protein. The existence of mixed spin states is not unusual [22] for the $[Fe_4S_4]^+$ clusters. The most common high-spin states mixing with the $S = ½$ state are $S = 3/2$ and $S = 7/2$, with the $S = 3/2$ state being the more common one. Because no signals of high-spin states can be observed in the EPR spectrum of Δ*nifB* NifEN, no spectral parameters of any high-spin state (e.g., *S*, *D*, *E/D*, or the relative percentage of a high-spin state) can be obtained. As such, it is extremely difficult to simulate the data and determine the exact origin of the nesting in Fig. 3 or the percentage contribution of any high-spin state. Only a range of acceptable parameters can be obtained. Assuming an additional contribution from only an $S = 3/2$ state, we could construct acceptable simulations (not shown) with the range of parameters as follows: 10–30% $S = 3/2$, $D = 4.5 \pm 2.5\ cm^{-1}$, $E/D = 0.10 \pm 0.10$, and 5% linear, temperature-independent *B* term, where the remaining 65–85% comes from the $S = ½$ state. An example of such a simulation is shown in red in Fig. 3.

Another possible explanation for the nesting of the magnetization curves is the presence of a low-lying $S = 3/2$ spin state that becomes thermally populated at elevated temperatures. This explanation is consistent with the EPR spectrum, where the $S = ½$ signal has high concentration (approximately two spins per protein) and no high-spin signals are observed at low temperatures. Our data do not allow us to definitively distinguish between these two explanations.

When the MCD spectra of reduced Δ*nifB* NifEN, $NifEN^{Precursor}$, and $NifEN^{"FeMoco"}$ are compared, it is apparent that they differ from one another (Fig. 4). This observation is not surprising, as $NifEN^{Precursor}$ and $NifEN^{"FeMoco"}$ contain paramagnetic clusters (i.e., precursor and "FeMoco," respectively) [9, 12] in addition to the permanent $[Fe_4S_4]^+$-like clusters. Regardless of the differences, the "signature" inflections at 360, 396, 430, and 458 nm, which are associated with the permanent $[Fe_4S_4]^+$-like clusters in Δ*nifB* NifEN (see earlier), are also present in the spectra of $NifEN^{Precursor}$ and $NifEN^{"FeMoco"}$ (Fig. 4). This is consistent with the assumed presence of the same permanent $[Fe_4S_4]^+$-like clusters in all three forms of NifEN [8–10]. The fact that the sharp inflections occur at the same wavelengths in all three spectra implies that the permanent clusters in all three proteins have the same electronic properties and are unperturbed by the coexistence of the precursor or "FeMoco" in these proteins. This result is of particular importance, as it suggests that the MCD spectra of the precursor and "FeMoco" can be derived by subtracting the spectrum of Δ*nifB* NifEN from the spectra of $NifEN^{Precursor}$ and $NifEN^{"FeMoco"}$, respectively.

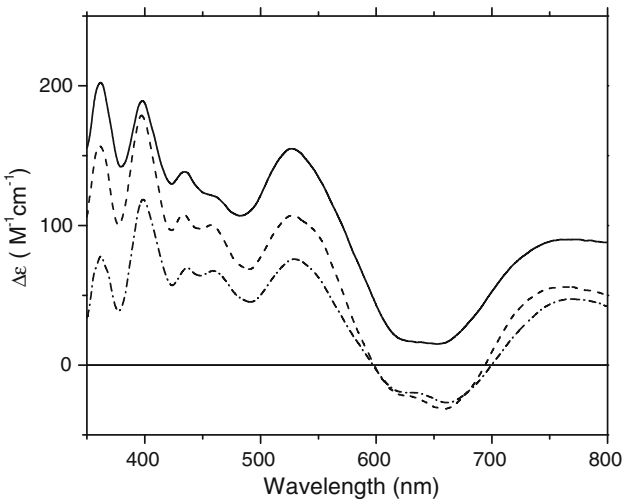

Fig. 4 Low-temperature (approximately 1.6 K) MCD spectra of Δ*nifB* NifEN (*dashed/dotted line*), $NifEN^{Precursor}$ (*dashed line*), and $NifEN^{"FeMoco"}$ (*solid line*) at 6 T

The difference spectra[1] between $NifEN^{Precursor}$ and Δ*nifB* NifEN (representing precursor) and between $NifEN^{"FeMoco"}$ and Δ*nifB* NifEN (representing "FeMoco"), which are corrected for depolarization effects, are shown in Fig. 5. The nearly complete elimination of the sharp inflections associated with the permanent $[Fe_4S_4]^+$-like cluster validates the subtraction procedure and implies that the resultant spectra arise solely from the protein-bound precursor or "FeMoco." Other than a positive baseline shift of the "FeMoco" spectrum relative to that of the precursor, there is an overall similarity of these two spectra. The origin of the positive spectral shift may be associated with the different spin states of these clusters (see below). The similarity of the spectral inflections suggests

[1] The difference spectra were constructed by subtracting data for Δ*nifB* NifEN from those for $NifEN^{Precursor}$ and $NifEN^{"FeMoco"}$, respectively. Since all data sets were taken from the saturation region of the magnetization (high field and low temperature), slight temperature differences between the data sets used for subtraction will not significantly affect the final spectrum. This is not the case with the magnetization data (see below).

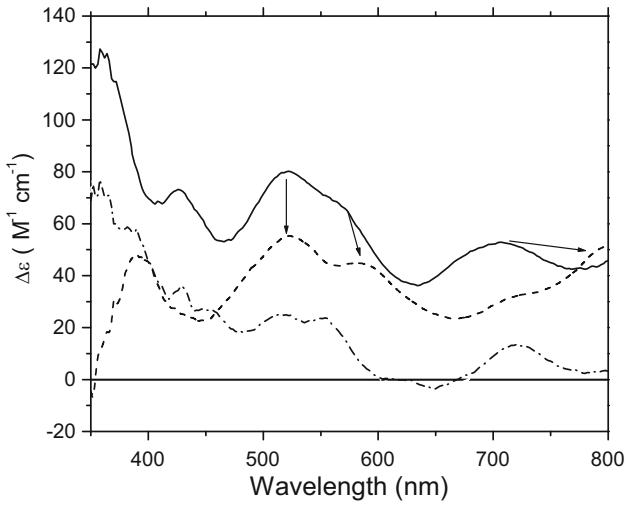

Fig. 5 MCD spectra of NifEN-bound precursor (*dashed/dotted line*), "FeMoco" (*solid line*), and MoFe-protein-bound FeMoco (*dashed line*) at 6 T and approximately 1.6 K. The spectra of the NifEN-bound precursor and "FeMoco" were derived by subtracting the spectrum of Δ*nifB* NifEN from the spectra of NifEN^{precursor} and NifEN$^{"FeMoco"}$, respectively, after correcting the spectra for sample depolarization. *Arrows* show the suggested inflection spectral shift between "FeMoco" in NifEN$^{"FeMoco"}$ and in the MoFe protein

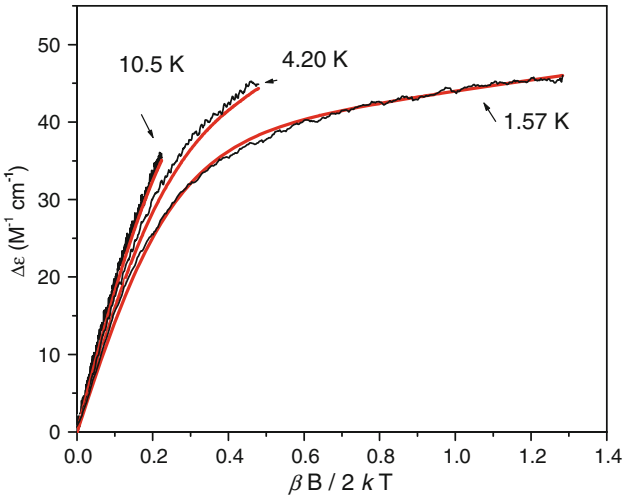

Fig. 6 Magnetization curves of "FeMoco" at 1.57, 4.20, and 10.5 K (*black*) and simulations of the magnetization curves (*red*) as an $S = 3/2$ system with $E/D = 0.056$ and $D = 6.5$ cm^{-1} (polarizations used in simulations $M_{xy} = 0.4$, $M_{xz} = 0.8$, $M_{yz} = -0.4$; diamagnetic *B*-term contribution 2%). All magnetization curves were directly obtained at 596 nm

that the transition energies of the Fe/S core of the precursor and "FeMoco" are conserved and that the addition of Mo and homocitrate to the precursor (which leads to the formation of "FeMoco") does not produce a major perturbation of the spectral parameters of the precursor. These observations are in excellent accord with our observation from our previous Fe K-edge XAS/EXAFS analysis of these two cluster species, which indicates a close resemblance in structure between the precursor and the "FeMoco" [9, 12].

Interestingly, the MCD spectrum of FeMoco in the reduced MoFe protein has a general shape similar to that of the spectra of the precursor and "FeMoco" in the reduced NifEN. However, the major spectral inflections of MoFe-protein-bound FeMoco above 500 nm appear to be shifted to longer wavelengths (Fig. 5). The spectral shift of the MoFe protein relative to NifEN$^{"FeMoco"}$ may reflect a different protein/solvation environment on FeMoco in NifEN and the MoFe protein. Part of this difference may originate from the difference in the coordination of the cluster in the two proteins. In MoFe protein, the Fe and Mo ends of FeMoco are ligated by αC275 and αH442, respectively; and the homocitrate entity of the cofactor is further coordinated by αK426 [3]. In NifEN, whereas the Fe-end ligand of the cofactor species is conserved as αC250, the Mo-end ligand and the homocitrate anchor are replaced by αN418 and αR402, respectively [23]. This change in ligand composition implies a weaker ligation of precursor or "FeMoco" in NifEN compared with that of FeMoco in the MoFe protein.

The magnetization data of the NifEN-associated precursor and "FeMoco" were subsequently analyzed to further investigate the electronic properties of both clusters. The best way to extract the magnetization data for a given cluster species in a mixture is to monitor the absorption of that cluster at a wavelength without the interference of other cluster species. However, this approach cannot be directly applied to the precursor, as there are no wavelengths where the MCD spectrum of NifEN^{Precursor} (originating from a mixture of the precursor and the permanent [Fe_4S_4]-like clusters) is nonzero while that of Δ*nifB* NifEN (originating only from the [Fe_4S_4]-like clusters) is zero (Fig. 4)—in other words, there are no wavelengths at which the spectrum of NifEN^{Precursor} arises solely from the precursor. As a result, the magnetization data of the precursor cannot be directly obtained and the only indicator of the spin state of this cluster is its EPR spectrum, which shows a dominant signal associated with an $S = ½$ state.[2] On the other hand, the MCD spectrum of NifEN$^{"FeMoco"}$ has positive inflections at 596 and 700 nm, where the spectrum of Δ*nifB* NifEN is zero (Fig. 4). Thus, the magnetization pattern of "FeMoco" can be directly monitored at these wavelengths (Fig. 6).

The directly measured magnetization curves of "FeMoco" (Fig. 6) can be closely simulated by an $S = 3/2$

[2] Since magnetization data have a strong temperature dependency, collecting data sets of both NifEN^{Precursor} and Δ*nifB* NifEN at the same temperature is problematic, especially at very low temperatures. It is difficult to poise both samples at the same temperature and a temperature fluctuation of ±0.1 K in the region of 1–4 K can result in a significant error.

system using the same spectral parameters derived for FeMoco in the MoFe protein ($E/D = 0.056, D = 6.5\ cm^{-1}$). This simulation is in good agreement with the presence of inflections in the $g = 3$–5 region of the EPR spectrum of NifEN$^{\text{"FeMoco"}}$ [12], which likely originate from the ground-state doublet of an $S = 3/2$ system ($g = 4.45$, 3.60; $E/D = 0.05$–0.10 and $D > 0$). The spread of the rhombicity, as well as the additional inflection at $g = 3.96$ ($E/D \sim 0$), suggests a small ensemble variation of the structure of "FeMoco" in NifEN. The weaker ligation of "FeMoco" in NifEN relative to that of the native cofactor in the MoFe protein [23] is likely the source of this spread of structures.

The positive shift of the MCD spectrum of "FeMoco" relative to that of the precursor (Fig. 5) is consistent with the difference in the EPR spin states of the precursor ($S = ½$) and "FeMco" ($S = 3/2$). It has been shown that increases in the spin states of a paramagnetic cluster can cause a positive baseline shift of its MCD spectrum [22]. Thus, despite the conservation of the core structure upon the conversion of the precursor to "FeMoco," the spin state of the cluster is altered, which reflects the impact of Mo and homocitrate on its electronic properties.

Conclusion

The overall outcome of the MCD investigation reported herein is consistent with that of the previous biochemical/spectroscopic analysis of the NifEN-bound clusters, yet it reveals additional electronic feature of these clusters unobserved by other spectroscopic approaches. With regard to the permanent $[Fe_4S_4]$-like cluster, the MCD spectrum of Δ*nifB* NifEN exhibits the inflections of a "classic," ferredoxin-type $[Fe_4S_4]^{+}$ cluster in the reduced state, whereas the magnetization curve constructed from this spectrum can be simulated by a dominant $S = ½$ system with a minor $S = 3/2$ component. These results are consistent with the previously observed $S = ½$ signal in the EPR spectrum of Δ*nifB* NifEN, although the high-spin component has not been reported previously. With regard to the NifEN-associate precursor and "FeMoco," their MCD spectra share a good deal of similarity with each other, despite a notable, positive shift of the "FeMoco" spectrum relative to the precursor spectrum, which is consistent with an increase in spin state from $S = ½$ (precursor) to $S = 3/2$ ("FeMoco"). More importantly, the MCD spectra of both the Precursor and the "FeMoco" on NifEN also resemble the spectrum of the FeMoco in the MoFe protein, suggesting a conservation of the basic Fe/S electronic structure in all of these clusters. This observation is particularly important, as it strengthens our previous hypothesis that the precursor has the complete core structure in place, that the conversion of the precursor to the "FeMoco" does not involve further rearrangement of the cluster structure, and that the "FeMoco" on NifEN is nearly identical in structure to the native cofactor in the MoFe protein. MCD analysis of the three NifEN species in the IDS-oxidized state is currently under way, which will facilitate the exploration of additional facets of the unique electronics of the NifEN-associated clusters.

Acknowledgments This work was supported by NIH Grant GM 67626 (M.W.R.) and NSF (2010)-Pfund-177 (B.J.H.).

References

1. Burgess BK, Lowe DJ (1996) Mechanism of molybdenum nitrogenase. Chem Rev 96:2983–3011
2. Georgiadis MM, Komiya H, Chakrabarti P, Woo D, Kornuc JJ, Rees DC (1992) Crystallographic structure of the nitrogenase iron protein from *Azotobacter vinelandii*. Science 257:1653–1659
3. Einsle O, Tezca FA, Andrade SLA et al (2002) Nitrogenase MoFe-protein at 1.16 Å resolution: a central ligand in the FeMo-cofactor. Science 297:1696–1700
4. Schindelin H, Kisker C, Schlessman JL, Howard JB, Rees DC (1997) Structure of ADP/AlF_4^- stabilized nitrogenase complex and its implications for signal transduction. Nature 22:370–376
5. Hu Y, Fay AW, Lee CC, Yoshizawa J, Ribbe MW (2008) Assembly of nitrogenase MoFe protein. Biochemistry 47:3973–3981
6. Dos Santos PC, Dean DR, Hu Y, Ribbe MW (2004) Formation and insertion of the nitrogenase iron–molybdenum cofactor. Chem Rev 104:1159–1173
7. Goodwin PJ, Agar JN, Roll JT, Roberts GP, Johnson MK, Dean DR (1998) The *Azotobacter vinelandiii* NifNE complex contains two identical [4Fe-4S] clusters. Biochemistry 37:10420–10428
8. Hu Y, Fay AW, Ribbe MW (2005) Identification of a nitrogenase FeMo cofactor precursor on NifEN complex. Proc Natl Acad Sci USA 102(9):3236–3241
9. Corbett MC, Hu Y, Ribbe MW, Hedman B, Hodgson KO (2006) Structural insights into a protein-bound iron–molybdenum cofactor precursor. Proc Natl Acad Sci USA 103:1238–1243
10. Hu Y, Corbett MC, Fay AW et al (2006) FeMo cofactor maturation on NifEN. Proc Natl Acad Sci USA 103(46):17119–17124
11. Hu Y, Corbett MC, Fay AW et al (2006) Nitrogenase Fe protein: a molybdatehomocitrate insertase. Proc Natl Acad Sci USA 103(46):17125–17130
12. Yoshizawa J, Blank MA, Fay AW et al (2009) Optimization of FeMoco maturation on NifEN. J Am Chem Soc 131:9321–9325
13. Burgess BK, Jacobs DB, Stiefel EI (1980) Large-scale purification of high activity *Azotobacter vinelandii* nitrogenase. Biochim Biophys Acta 614:196–209
14. Broach RB, Rupnik K, Hu Y et al (2004) VTVH-MCD spectroscopic study of the metal clusters in the Δ*nifB* and Δ*nifH* MoFe proteins of nitrogenase from *Azotobacter vinelandii*. Biochemistry 45:15039–15048
15. Bursey EH, Burgess BK (1998) The role of methionine 156 in cross-subunit nucleotide interactions in the iron protein of nitrogenase. J Biol Chem 273:29678–29685

16. Neese F, Solomon EI (1999) MCD C-term signs, saturation behavior, and determination of band polarizations in randomly oriented systems with $S \geq 1/2$. Applications to $S = 1/2$ and $S = 5/2$. Inorg Chem 38:1847–1865
17. Conover RC, Kowal AT, Fu W et al (1990) Spectroscopic characterization of the novel iron–sulfur cluster in *Pyrococcus furiosus* ferredoxin. J Biol Chem 265(15):8533–8541
18. Werth MT, Tang S-F, Formicka G, Zeppezauer M, Johnson MK (1995) Magnetic circular dichroism and electron parmagnetic resonance studies of cobalt-substituted horse liver alcohol dehydrogenase. Inorg Chem 34:218–228
19. Fu W, O'Handley S, Cunningham RP, Johnson MK (1992) The role of the iron–sulfur cluster in *Escherichia coli* endonuclease III. J Biol Chem 267(23):16135–16137
20. Crouse BR, Meyer J, Johnson MK (1995) Spectroscopic evidence for a reduced Fe_2S_2 cluster with a $S = 9/2$ ground state in mutant forms of *Clostridium pasteurianum* 2Fe ferredoxin. J Am Chem Soc 117:9612–9613
21. Johnson MK, Robinson AE, Thomson AJ (1982) Low-temperature magnetic circular dichroism studies of iron–sulfur proteins. In: Spiro TG (ed) Iron–sulfur proteins. Wiley, New York, pp 367–406
22. Onate YA, Finnegan MG, Hales BJ, Johnson MK (1993) Variable temperature magnetic circular dichroism studies of reduced nitrogenase iron proteins and $[4Fe\text{-}4S]^+$ synthetic analog clusters. Biochim Biophys Acta 1164:113–123
23. Hu Y, Ribbe MW (2010) Decoding the nitrogenase mechanism: the homologue approach. Acc Chem Res 43(3):475–484